Imaging cancer cell therapy: Ponomarev provides an overview of direct and indirect cell labeling for nuclear imaging of transferred cells, with a focus on reporter gene applications that allow visualization of cellular trafficking, persistence, proliferation, and function. . . . . ***Page 1013***

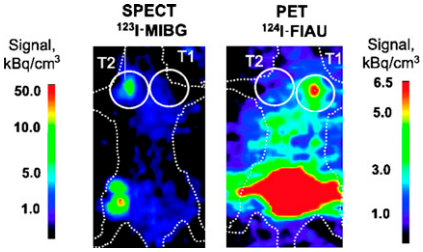

Targeting "oncogene addiction": Reilly offers perspective on therapeutic strategies aimed at disrupting the influence of the *HER2* oncogene and previews an article in this issue of *JNM* that proposes a combined imaging assessment and targeted therapy approach. . . . . ***Page 1017***

Dose painting in head and neck cancer: Dirix and colleagues evaluate the potential of functional imaging with ^{18}F-FDG PET, ^{18}F-fluoromisonidazole PET, diffusion-weighted MRI, and dynamic contrast-enhanced MRI to provide an accurate biologic target for dose painting in radiotherapy. . . . . ***Page 1020***

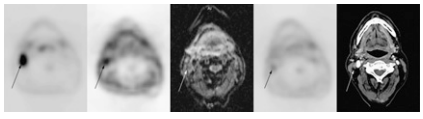

^{18}F-FLT kinetics in head and neck cancer: Menda and colleagues investigate the kinetic behavior of this PET tracer before and early after initiation of chemoradiation therapy in patients with squamous cell head and neck cancer. . . . ***Page 1028***

PET in colorectal liver metastasis: Ruers and colleagues determine whether the addition of ^{18}F-FDG PET to conventional staging in colorectal liver metastases leads to improved clinical management, especially in the selection of appropriate patients for laparotomy. . . . . ***Page 1036***

SPECT/CT for diabetic foot infection: Filippi and colleagues assess the role of SPECT/CT ^{99m}Tc-HMPAO–labeled leukocyte scanning in diagnosing diabetic foot infection, differentiating between bone and soft-tissue involvement, and defining extent of disease. . . . . ***Page 1042***

Quantification of ^{18}F-PBR06 in brain: Fujimura and colleagues evaluate the ability of a novel PET tracer to quantify translocator proteins, which are valid biomarkers of inflammation, in the human brain. . . . . ***Page 1047***

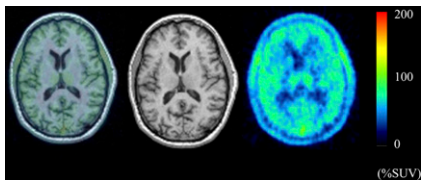

Frontocerebellar dissociation in mild TBI: Hattori and colleagues investigate the brain activation of regional cerebral blood flow during a psychological test in patients with mild traumatic brain injury to explore underlying mechanisms of cognitive fatigue. . . . . ***Page 1054***

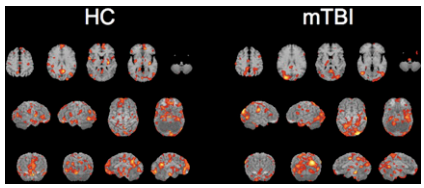

Accuracy of ^{82}Rb PET: El Fakhri and colleagues introduce an analytic method for determining the accuracy and reproducibility of myocardial blood flow assessment using ^{82}Rb cardiac PET. . . . . ***Page 1062***

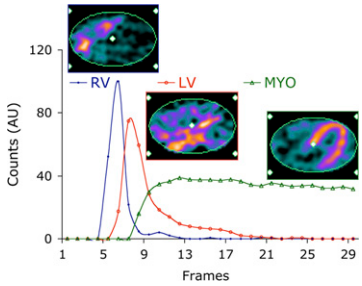

Tumor-to-brain communication: Golan and colleagues compare brain metabolism in patients with and without lung cancer to determine whether the brain receives stimuli from tumors and, in turn, acts to modulate tumor progression. . . . . ***Page 1072***

Quantification of myocardial blood flow: Camici and Rimoldi provide an educational overview of the ability of myocardial blood flow measurement to offer unique diagnostic information about the coronary microcirculation and serve as a surrogate endpoint in therapy studies. . . . ***Page 1076***

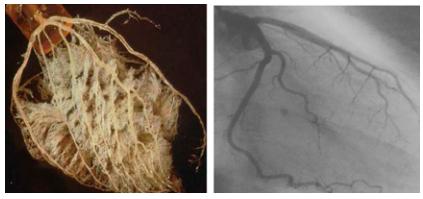

Cell imaging with PET and MRI: Higuchi and colleagues explore the feasibility of combined ^{124}I PET and iron oxide MRI for monitoring cell engraftment and survival after cell transplantation. . . . . ***Page 1088***

Quantifying biomarkers in the brain: Miyoshi and colleagues describe a method to quantify ^{11}C-AC-5216 binding in the human brain and discuss this tracer's potential as a PET radioligand and biomarker for inflammation in the brain and neurodegenerative disorders. . . . . ***Page 1095***

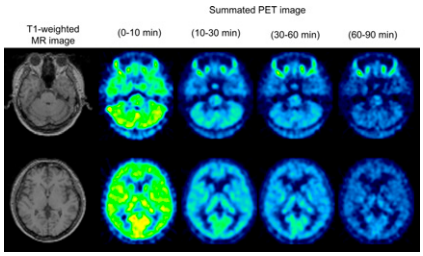

^{18}F-FDG and ^{18}F-FLT kinetics after therapy: Brepoels and colleagues compare these tracers as markers of proliferation early after cytotoxic therapy and provide evidence of the importance of drug-specific responses in the use of PET as a prognostic tool. . . . . ***Page 1102***

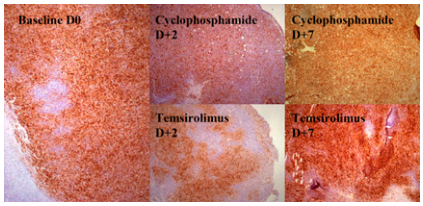

Molecular imaging of pulmonary hypertension: Dupuis et al. describe the development of a ^{99m}Tc-labeled linear adrenomedullin derivative for imaging of pulmonary circulation and present results from initial kinetic and imaging studies in rats. . . . . ***Page 1110***

Imaging EGFR antibody distribution: Niu and colleagues use PET to investigate the in vivo kinetics of antibody delivery and localization of ^{64}Cu-labeled panitumumab, an epidermal growth factor receptor–targeting monoclonal antibody with promise in head and neck squamous cell carcinoma. . . . . ***Page 1116***

Immunoimaging of CXCR4 expression: Nimmagadda and colleagues report on assessment of chemokine receptor 4 expression levels in experimental brain tumors using ^{125}I-labeled monoclonal antibody SPECT/CT. . . . . ***Page 1124***

PET and *HER2* expression: Kramer-Marek and colleagues describe studies with an Affibody molecule to assess human epidermal growth factor receptor type 2 expression and monitor possible changes in receptor status after *HER2*-targeted therapies. . . . . ***Page 1131***

Abcc2* and ^{99m}Tc-mebrofenin:** Bhargava and colleagues explore the specific molecular transporter mechanisms directing bile canicular transport of this ^{99m}Tc-labeled organic anion and its analogs. . . . . ***Page 1140

^{123}I-FP-CIT binding after haloperidol: Nikolaus and colleagues use small-animal SPECT and a dopamine transporter radioligand to assess the effects of this common antipsychotic medication on synaptic dopamine. . . . . ***Page 1147***

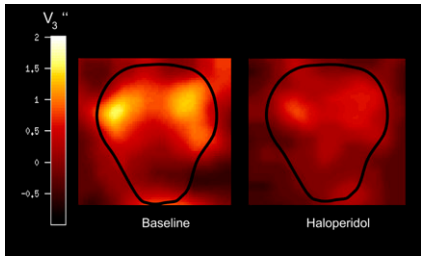

α-particle RIT of ovarian cancer: Andersson and colleagues report on the pharmacokinetics of a ^{211}At-labeled monoclonal antibody as part of a phase 1 study to determine its efficacy and safety in treating microscopic ovarian cancer tumor clusters. . . . . ***Page 1153***

Differential thyroid stunning: Lundh and colleagues study effects on iodide transport and sodium iodide symporter mRNA expression in thyrocytes exposed to ^{123}I, ^{131}I, ^{99m}Tc, and ^{211}At. . . . . ***Page 1161***

^{64}Cu-RGD-bombesin PET: Liu and colleagues describe the development and experimental evaluation of this novel heterodimer for dual integrin $\alpha_v\beta_3$- and gastrin-releasing peptide receptor–targeted imaging. . . . . ***Page 1168***

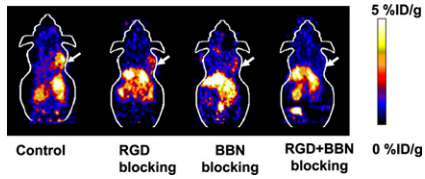

In-line protein radiolabeling: Harris and colleagues present proof-of-principle studies using a novel method for rapidly radiolabeling commercial amounts of protein without compromising binding potency or structural integrity. . . . . ***Page 1178***

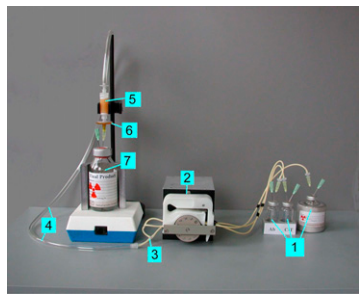

ACRIN PET qualification: Scheuermann and colleagues describe American College of Radiology Imaging Network PET Core Laboratory processes for qualification of sites to participate in multicenter research trials and focus on the importance of accurate SUV calibrations. . . . . ***Page 1187***

ON THE COVER

Chemokine receptor 4 is expressed at a higher level in neoplastic tissue than in normal tissue and is a possible predictive marker of metastatic potential. The feasibility of imaging chemokine receptor 4 expression in experimental brain tumors has been shown. SPECT/CT with a ^{125}I-labeled monoclonal antibody demonstrated a clear and specific accumulation of radioactivity in the tumors by 24 hours.

See page 1128.